J. Fluid Mech. (1967), *vol.* 27, *part* 3, *pp.* 541–549
Printed in Great Britain

Some experiments on equilibrium turbulent boundary layers in favourable pressure gradients

By H. J. HERRING AND J. F. NORBURY†
Department of Aerospace and Mechanical Sciences, Princeton University, Princeton, N.J.

(Received 16 July 1965 and in revised form 18 July 1966)

A wind tunnel in which an arbitrary negative pressure gradient could be developed has been built for boundary-layer studies. The effects of selected pressure gradients on boundary layers grown on one of the walls of the tunnel were studied. It was possible to obtain equilibrium boundary layers of the type first suggested by Clauser: that is, layers whose non-dimensional velocity-defect distribution is invariant along the direction of flow. The velocity-defect distributions for two such boundary layers were established, corresponding to values of Clauser's dimensionless pressure-gradient parameter β of $-0{\cdot}35$ and $-0{\cdot}53$. These velocity profiles are compared with the profiles predicted theoretically by Mellor & Gibson (1966). The agreement between the two is very good.

1. Introduction

The dimensionless velocity-defect function representing the outer part of a boundary layer has the form

$$f'(\eta) = (U-u)/u_\tau,$$

where U = free-stream velocity, u = velocity in x-direction, and u_τ, the friction velocity, is $(\tau_w/\rho)^{\frac{1}{2}}$, τ_w being the wall shear stress and ρ the density. η is the dimensionless wall distance, y/Δ, where Δ, the defect displacement thickness, is defined as

$$\int_0^\infty (U-u)/u_\tau \, dy.$$

It is well established that $f'(\eta)$ is independent of Reynolds number for a constant-pressure turbulent boundary layer, so that its form does not change along the layer. There are certain variable pressure boundary layers which also have this property, and Clauser (1956) called these equilibrium layers. He further reasoned that the pressure gradient, expressed in some dimensionless form, must have a constant value in an equilibrium layer, and that to each value of the dimensionless pressure gradient would correspond a particular form of the function $f'(\eta)$. Clauser built a wind-tunnel designed for positive pressure gradients and was able to measure equilibrium profiles corresponding to two particular positive gradients. Using these data, he concluded that the dimensionless form of pressure gradient which was most nearly constant for each equilibrium profile

† Present address: Department of Mechanical Engineering, University of Liverpool.

was $(\delta^*/\tau_w)\,\partial p/\partial x$, denoted by β. In this expression δ^* is the boundary-layer displacement thickness and p is the pressure. The two values of β for which Clauser obtained profiles were 1·8 and 8.

Little work has been done on turbulent boundary layers in negative pressure gradients, especially on equilibrium boundary layers. Therefore it was the purpose of this study to show that equilibrium boundary layers as defined do exist in this flow regime, and to establish the form of the function $f'(\eta)$ for several values of β.

Recently, an advance has been made toward the theoretical calculation of turbulent boundary-layer profiles. Mellor & Gibson (1966), drawing upon some of the work of Clauser, have developed a method for solving the equations of motion in the range of equilibrium pressure gradients for which $-0{\cdot}5 \leqslant \beta \leqslant \infty$. This method yields theoretical solutions for $f'(\eta)$, the equilibrium velocity profile. These theoretical results agree very well with the experimental velocity profiles of Clauser (1954) and Stratford (1959), obtained in positive pressure gradients. In the present paper it will be shown that the agreement between theory and experiment is also very good in the case of negative pressure gradients.

2. Apparatus

An open return wind tunnel was designed especially for the experiment. Immediately behind the entry scroll were placed a honeycomb and two screens to provide uniform flow. These were followed by a section of constant cross-sectional area in which the boundary layer developed to a displacement thickness of between 0·12 and 0·15 in. at the beginning of the working section. Reynolds numbers for the flow may be determined from the fact that $U/\nu = 37{,}500\,\text{in.}^{-1}$ at this point. The test wall in the working section was a milled aluminium plate of $\frac{1}{2}$ in. thickness mounted vertically; the opposite wall was a flexible masonite sheet, and the horizontal side walls were of Plexiglas. A wide range of favourable pressure gradients could be produced in the working section by setting the shape of the flexible wall with adjusting screws. The working section was 8 ft. long but the pressure distribution could not be completely controlled over the whole of this distance, so that the useful length of the test wall was about 50 boundary-layer thicknesses. Thus, if the layer could be brought to equilibrium in about 20 thicknesses, it would be held in equilibrium for about 30 more thicknesses.

Provision was made for measuring the velocity profile at intervals of 1 ft. along the whole working section. The measurement was made with a small goose-necked Pitot tube inserted through the aluminium test wall. The opening of this Pitot tube was 0·004 in. high and 0·050 in. wide, and the overall height of the tip was 0·007 in. The aluminium plate was vertical so that the apparatus for traversing the Pitot tube was much more accessible than it would have been on the bottom or on the top of the test section. Furthermore, the direction of gravity provided a reference for the yawmeter, which was used to check the uniformity of the flow direction. The yawmeter could be mounted in any of the Pitot-traverse stations, and a spirit level attached to it could then be used to determine its inclination.

No boundary-layer control was provided on the side walls. However, owing to the favourable pressure gradient in the test section, the boundary layers on the side walls remained about 1·5 in. thick. The influence of these layers on the centre third of the 30 in. wide test wall was found to be negligible.

3. Experimental problems and limitations

Considerable attention was paid to the problem of maintaining two-dimensional flow in the boundary layer occupying the central part of the test wall in the working section, and all joints in the tunnel structure were carefully sealed to prevent leakage.

The most difficult problem was posed by the vortex which at first formed on the floor near to the entrance to the wind tunnel. A household fan was placed under the entry to the tunnel to blow the vortex away. The effect of the fan was to weaken the vortex greatly, and to move it much farther from the tunnel entry. Such streamwise vorticity as remained was attenuated by the honeycomb and screens, and experimental checks revealed that any cross-flows in the measured part of the boundary layer were acceptably small.

The two-dimensionality of the boundary layer was checked in three ways: (i) by yawmeter measurements; (ii) by carrying out additional velocity traverses at stations located 6 in. off the centre-line of the test wall; (iii) by checking values of terms in the boundary-layer momentum equation. The yawmeter traverses were carried out at a number of stations along the measured boundary layer and showed a maximum variation in direction of less than 1°. The velocity traverses showed that, over the central 12 in. of the test wall, the span-wise variation in velocity was less than 1 % of the local value.

In the experimental realization of equilibrium boundary layers in a favourable pressure gradient, the design of the wind tunnel imposes restrictions on both the portion of the flow along which the pressure gradient may be enforced and the maximum pressure drop which may be created by accelerating the flow. Because of the first limitation, it is important to make the best use of that space in which the pressure gradient is enforced. The sooner that the profile can be brought to equilibrium, the longer the distance over which it can be kept in equilibrium. It was found that the fastest way to bring the profile into equilibrium was to set the pressure gradient to produce a much higher β and then to revert to the proper β when the development was approximately complete. Figure 1 shows the variation of the quantities $(\delta^*\tau_{w0}/\delta_0^*\tau_w)$ and $\beta(\delta_0^*\tau_w/\delta^*\tau_{w0})$ along the two experimental boundary layers. The manner in which the layers attain equilibrium is illustrated by the way in which the points approach and join the rectangular hyperbolae corresponding to constant β. The pressure distributions required to accomplish this are shown in figure 2.

However, the use of a high initial pressure gradient is limited by the fixed maximum pressure drop. For one thing, these initially higher pressure gradients use up the available pressure drop faster. But, more than that, they reduce the boundary-layer thickness more rapidly, and, since $dp/dx \simeq 1/\delta^*$ (for a given β), an even higher pressure gradient is necessary when the layer is finally to be kept

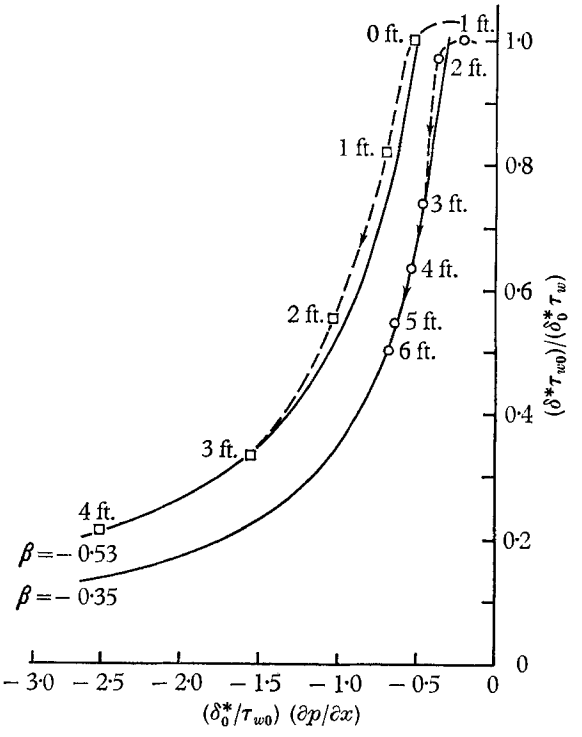

FIGURE 1. The approach to equilibrium on the β-plane. The dashed lines are the actual paths of the boundary layer. The solid lines are lines of constant β.

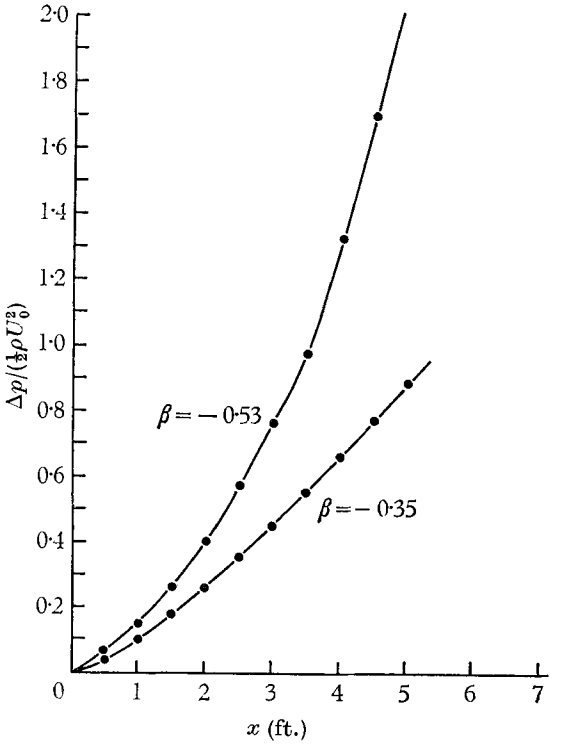

FIGURE 2. Pressure distribution required to bring boundary layer to equilibrium and maintain it in equilibrium.

in equilibrium. Because of these limitations it was not possible to determine whether equilibrium profiles can exist at values of β substantially lower than about $-0{\cdot}5$, which is the limiting value predicted by the Mellor–Gibson theory. (The precise limit is slightly dependent on Reynolds number.) A small increase in the dimensions of the tunnel would not have been enough to make possible a study of the lower bound on β for equilibrium profiles, since a large increase in both equilibration distance and pressure drop would be necessary to lower β by even a small amount.

4. Results

Equilibrium velocity profiles were obtained for two values of β. It was possible to maintain one boundary layer in equilibrium for a distance of 36 boundary-layer thicknesses at $\beta = -0{\cdot}35$. Another boundary layer, with $\beta = -0{\cdot}53$, could

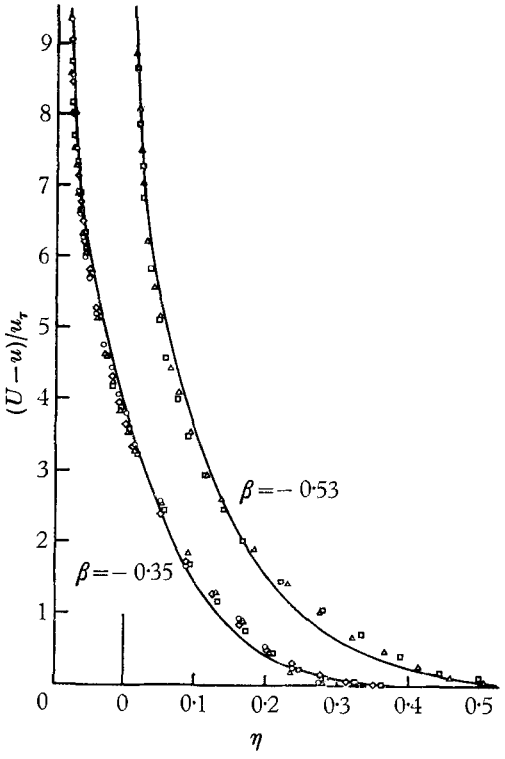

FIGURE 3. Equilibrium defect profiles for the two cases studied shown with the profiles predicted by the Mellor–Gibson (1966) theory. ○, $x = 2$ ft.; △, $x = 3$ ft.; □, $x = 4$ ft.; ◇, $x = 5$ ft.; —, Mellor–Gibson.

not be brought to equilibrium until near the end of the test section, owing to the experimental limitations mentioned above, and it was kept in equilibrium for a distance of 10 boundary-layer thicknesses. These two profiles are plotted in figure 3 in the form $(U-u)/u_\tau$ against y/Δ. In figure 3 the non-dimensional wall distance is expressed as y/Δ rather than y/δ because of the greater accuracy with which Δ can be measured experimentally. For a given value of β, δ is proportional

to Δ, and, when the equilibrium profile has been established, the ratio of the two is fixed. For comparison, the profiles predicted by the theory of Mellor & Gibson are also shown in figure 3. The correspondence between the theoretical and

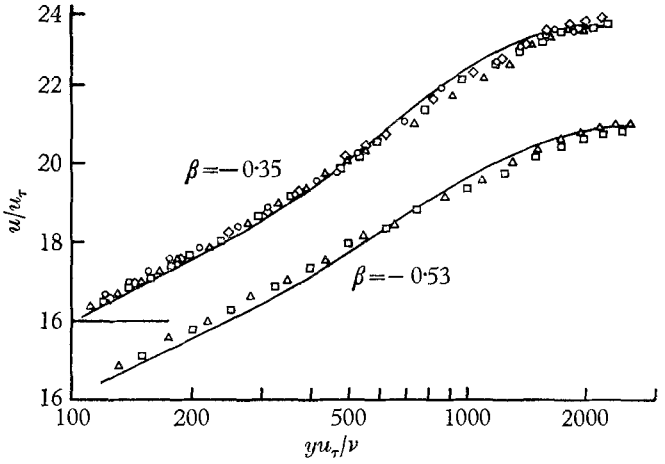

FIGURE 4. Equilibrium profiles for the two cases studied plotted in the 'law of the wall' form shown with the profiles predicted by the Mellor–Gibson (1966) theory (solid line). ○, $x = 2$ ft.; △, $x = 3$ ft.; □, $x = 4$ ft.; ◇, $x = 5$ ft.

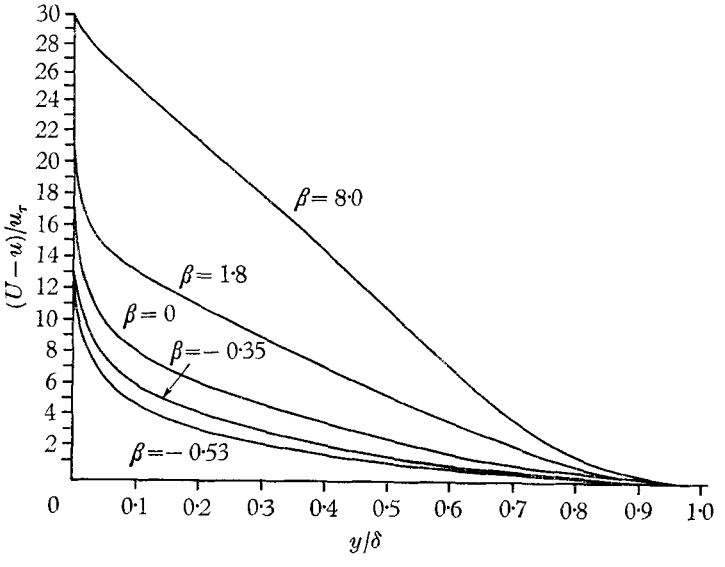

FIGURE 5. Equilibrium defect profiles obtained by Clauser (1954) compared with those of the present experiments.

experimental profiles is clearly very good, similar to that for Clauser's and Stratford's data shown in Mellor & Gibson's (1966) paper. This indicates that their empirical assumptions, which were made primarily on the basis of studies in zero and positive pressure gradients, hold equally well for negative values of β. Therefore, the validity of the theory would appear to extend over the entire range of equilibrium boundary layers ($-0{\cdot}5 \leqslant \beta \leqslant \infty$). The experimental and

theoretical velocity profiles are plotted in figure 4 with co-ordinates u/u_τ and yu_τ/ν. This plot emphasizes the relation between the two close to the wall.

The characteristics of the profiles in part of the range of β are shown well by plotting the results obtained above with Clauser's profiles for values of β of 1·8 and 8·0 (see figure 5). Here it is clear that the trend in the shape of the velocity profiles begun in the regime of positive β carries smoothly into the regime of negative β. For a comparison of this type, the co-ordinate y/δ is the best choice of independent variable.

The defect shape factor G is defined as

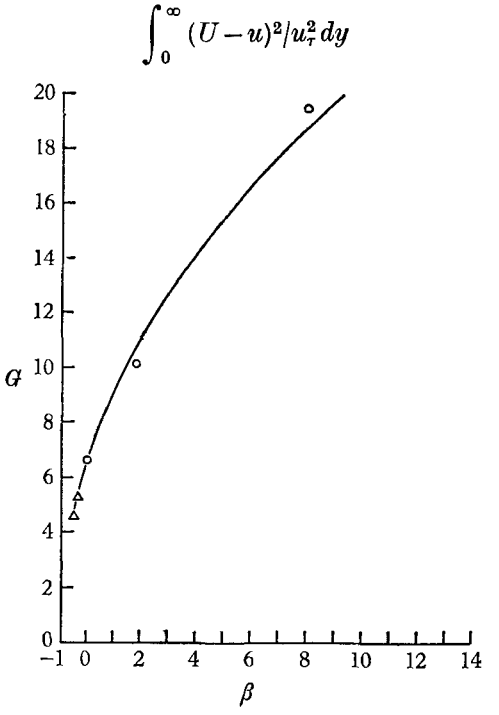

FIGURE 6. The defect shape factor, G, predicted by the Mellor–Gibson (1966) theory compared with values obtained by Clauser (1954) and those of the present experiment. ○, Clauser; △, present results.

and its variation with β is shown in figure 6 for both the present values and those obtained by Clauser. In view of the close correspondence between the experimental velocity profiles and those predicted by Mellor & Gibson's theory, it is not surprising to find that the experimental values of G lie on the theoretical curve. For $\beta = -0{\cdot}35$ and $-0{\cdot}53$, the theoretical prediction for G matches the experimental to two significant figures. Another parameter used in the theory is the defect constant, $A(\beta)$, which is defined by

$$A(\beta) = \lim_{\eta \to 0} [f'(\eta, \beta) - (1/\kappa)\log_e \eta],$$

and which appears in the skin-friction equation

$$(U/u_\tau) = 1/\gamma = (1/\kappa)\log_e (U\delta^*/\nu) + A(\beta) + B.$$

As may be seen in figure 7, the experimental results again support the theory quite well.

The comparison between experiment and theory may be carried a stage further. In principle it is possible to examine the major experimental assumption of the theory, namely the form of the eddy viscosity function. However, the

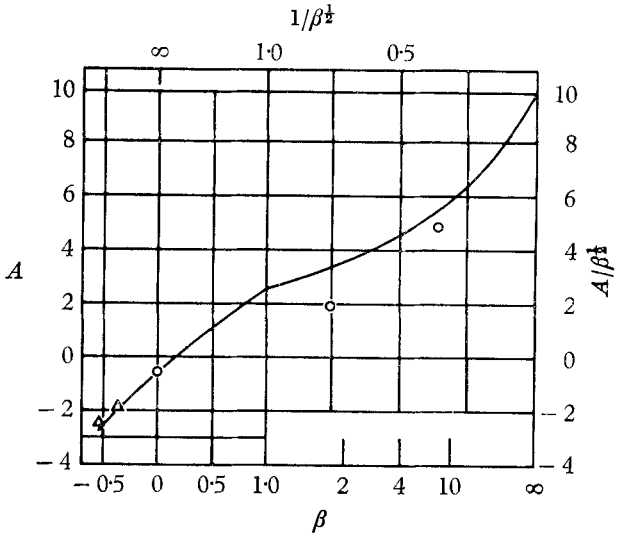

FIGURE 7. The defect constant, $A(\beta)$, predicted by the Mellor–Gibson (1966) theory compared with values obtained from Clauser's (1954) profiles and those of the present experiment. ○, Clauser; △, present results.

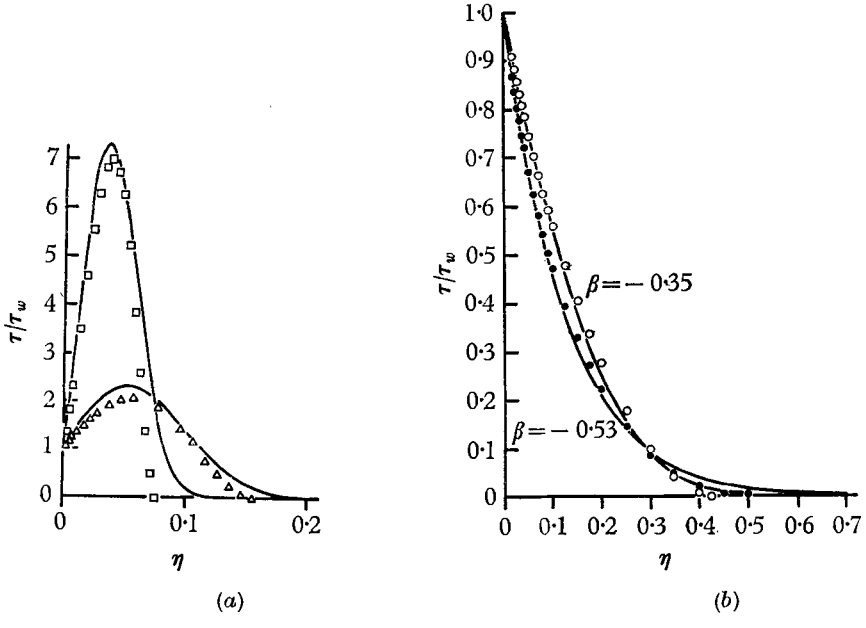

FIGURE 8. The shear stress from the Mellor–Gibson (1966) theory compared with the shear stress found from (*a*) Clauser's profiles, and (*b*) the present experiment, using equation 14′ from Mellor–Gibson (1966). □, $\beta = 8{\cdot}0$; △, $\beta = 1{\cdot}8$; ○, $\beta = -0{\cdot}35$; ●, $\beta = -0{\cdot}53$.

direct determination of eddy viscosity would require numerical differentiation of the velocity profiles, and is therefore liable to be inaccurate. It is preferable to compare the distribution of non-dimensional shear stress, τ/τ_w, calculated using Mellor & Gibson's form of the momentum equation (1966, equation (14)), with the curves obtained on the basis of the Mellor–Gibson eddy viscosity function.

The results for Clauser's profiles are given in figure 8(*a*) and those for the present experiments in figure 8(*b*). In both cases the agreement between experimental and theoretical curves is very good.

The work was carried out under the Bureau of Ships Fundamental Hydromechanics Research Programme, S-R 00901 01, administered by the David Taylor Model Basin; contract Nonr.-1858(38).

REFERENCES

CLAUSER, F. 1954 Turbulent boundary layers in adverse pressure gradients. *J. Aero. Sci.* **21**, 91–108.

CLAUSER, F. 1956 The turbulent boundary layer. *Adv. Appl. Mech.* **4**, 1–51.

MELLOR, G. L. & GIBSON, D. M. 1966 Equilibrium turbulent boundary layers. *J. Fluid Mech.* **24**, 225–253.

STRATFORD, B. S. 1959 An experimental flow with zero skin friction throughout its region of pressure rise. *J. Fluid Mech.* **5**, 17–35.